Optimizing the shape parameters of radial basis functions: an application to automobile crashworthiness

E Acar
Department of Mechanical Engineering, TOBB University of Economics and Technology, Söğütözü Caddesi No: 43, Söğütözü, Ankara, Turkey. email: acar@etu.edu.tr

The manuscript was received on 17 March 2010 and was accepted after revision for publication on 4 June 2010.

DOI: 10.1243/09544070JAUTO1560

Abstract: Radial basis functions (RBFs) are approximate mathematical models that can mimic the behaviour of rapidly changing and computationally expensive simulations, such as finite element simulations for predicting automobile crash responses. The most popular way of selecting optimal RBF shape parameters is based on minimizing the *global* cross-validation error (CVE). Solving this optimization problem may lead to the construction of globally accurate RBF models, but the shape parameters are assumed to be constant over the entire design space. On the other hand, having flexible shape parameters that can change over the design space may allow the local behaviour to be captured better, thereby improving the accuracy. Thus, optimizing the RBF shape parameters based on minimization of the *pointwise* CVE rather than the global CVE is proposed in this paper. Three benchmark mathematical functions followed by an automobile crash problem are used to evaluate the effectiveness of the proposed method. It is found that the RBF models based on the minimum pointwise CVE outperform the RBF models based on the minimum global CVE.

Keywords: optimization, shape parameters, radial basis functions, automobile crashworthiness

1 INTRODUCTION

Radial basis functions (RBFs) are approximate mathematical models used as surrogates for rapidly changing and computationally expensive simulations. RBFs have many attractive features including, first, their capability of accurately modelling arbitrary functions, second, their capability of handling scattered training points in multiple dimensions, and, third, their relatively simple implementation compared with kriging and neural networks [**1**]. Because of these capabilities, RBFs have been used in many engineering applications. Hardy [**2**–**4**] used RBFs to predict the potential or temperature on the Earth's surface at some desired points. Arad *et al.* [**5**] used RBFs for image warping of facial expressions. Tu and Barton [**6**] used RBFs as surrogates for electronic circuit simulation models. Zala and Barradole [**7**] used RBFs to warp aerial photographs to orthomaps. Kremper *et al.* [**8**] used RBFs in neurophysics applications to classify neural signals. Papila *et al.* [**9**] used RBFs for design optimization of a propulsion system and turbomachinery components. Reddy and Ganguli [**10**] used RBFs to predict structural damage in helicopter rotor blades. Lai *et al.* [**11**] used RBFs for gear fault classification. Sonar *et al.* [**12**] used RBFs for predicting the surface roughness in a turning process. Zhang *et al.* [**13**] used RBFs for optimizing a microelectronic packaging system. Young *et al.* [**14**] used RBFs to predict the responses of control systems used in aircraft. Sjögren [**15**] used RBFs for the multi-objective design of antennae.

RBFs have also attracted the attention of several researchers to predict the crash performances of vehicles and their components. Jin *et al.* [**16**] used RBFs for predicting the rollover characteristics of a trailer analysed by Chen *et al.* [**17**]. They constructed four different surrogate model types (polynomial regression (PR), multi-variate adaptive regression splines, RBF, and kriging) and found that the RBF model was the most accurate. Lanzi *et al.* [**18**] constructed RBFs to approximate crash capabilities of composite absorbers to perform multi-objective

shape optimization of the absorbers under crashworthiness requirements. Hamza and Saitou [**19**] used RBFs to design the B-pillar of an automobile under roof crash conditions. They constructed PR, neural network, and RBF models to predict the maximum crush force and found that the RBF model was the most accurate. Fang *et al.* [**20**] utilized RBFs to perform multi-objective optimization of automobile components for crashworthiness. They constructed PR and RBF models to approximate the energy absorption and peak acceleration responses of an automobile and found that the RBF model was more accurate than the PR model. Yang *et al.* [**21**] constructed RBF models for vehicle frontal-impact simulations. They constructed five different surrogate types (PR, moving least-squares, kriging, RBF, and adaptive and interactive modelling system models) and found that the RBF model was the most accurate surrogate type. Last but not least, Rais-Rohani *et al.* [**22**] used RBFs to perform reliability-based optimization of the front side-rail component of a passenger car under full-frontal- and offset-frontal-crash scenarios.

The accuracy of the constructed RBF models depends heavily on the procedure followed to select the RBF shape parameters. Several methods have been suggested in the literature for selecting the shape parameters. Hardy [**2**], Franke [**23**], Kansa [**24**, **25**], and Fasshauer [**26**] proposed empirical formulations for selecting good values for the shape parameters. Carlson and Foley [**27**] and then Foley [**28**], with an improved procedure, proposed computing the RBF shape parameters by minimizing the r.m.s. error (RMSE) evaluated at a set of test points. In these two studies, several RBF models were built for different values of the shape parameters using a common set of training points, and the accuracies of the constructed RBF models were evaluated for a dense grid of test points. Finally, the shape parameters corresponding to the minimum RMSE were selected. These procedures require the use of a fine grid of test points, and so it is computationally prohibitive when the responses are calculated through time-consuming analysis models (e.g. high-fidelity finite element (FE) simulations). Rippa [**29**] proposed computing the RBF shape parameters by minimizing the r.m.s. cross-validation error (CVE) evaluated at training points. The procedure employed by Rippa [**29**] is more advantageous than the procedures used by Carlson and Foley [**27**] and Foley [**28**] as it does not require a set of test points. However, evaluation of the CVE becomes computationally costly when the number of training points is large. To resolve this computational challenge, Wang [**30**] and later Roque and Ferreira [**31**] proposed more efficient ways to compute the CVE and minimized the r.m.s. CVE to select the RBF shape parameters. However, it should be noted that, within the context of crashworthiness analysis, the computational cost of CVE evaluation is much smaller than a single crash simulation for a moderate number of variables.

The accuracy of RBF models can be further improved by allowing the RBF shape parameters to take variable values over the design space. Having flexible shape parameters may allow the local behaviour to be captured better, thereby improving the accuracy. This can be easily achieved by allowing the shape parameters to take different values at any different training points. However, as the number of training points increases, the computational cost associated with optimization of the shape parameters can quickly escalate. Hence, this is not a good strategy. This paper proposes an efficient optimization procedure for selecting flexible RBF shape parameters. The proposed formulation is applied to three benchmark problems followed by application to an automobile crash problem.

The remainder of the paper is organized as follows. Section 2 provides a brief description of the RBFs. Section 3 presents the current practice in choosing the RBF parameters. A new formulation to choose the RBF parameters is proposed in section 4. Three benchmark mathematical problems and an automobile crash problem used to measure the accuracy of the proposed method are presented in section 5. The numerical procedure followed is detailed in section 6. The results of test problems are presented and discussed in section 7, followed by concluding remarks given in section 8.

2 BRIEF DESCRIPTION OF THE RBF

The RBFs were originally developed to approximate multi-variate functions based on scattered data [**32**]. For a data set consisting of the values of the input variables and response values at N training points, the true function $y(\boldsymbol{x})$ can be approximated as

$$\hat{y}(\boldsymbol{x}) = \sum_{k=1}^{N} \lambda_k \phi(\|\boldsymbol{x} - \boldsymbol{x}_k\|) \tag{1}$$

where $\boldsymbol{x}$ is the vector of input variables, $\boldsymbol{x}_k$ is the vector of input variables at the kth training point, $\|\boldsymbol{x} - \boldsymbol{x}_k\| = \sqrt{(\boldsymbol{x} - \boldsymbol{x}_k)^{\mathrm{T}}(\boldsymbol{x} - \boldsymbol{x}_k)}$ is the Euclidean norm

representing the radial distance from the prediction point $\boldsymbol{x}$ to the training point $\boldsymbol{x}_k$, ϕ is a radially symmetric basis function, and λ_k are the unknown interpolation coefficients. Equation (1) represents a linear combination of a finite number of radially symmetric basis functions. The most popular RBF formulations include $\phi(r)=r^2\log(r)$ (thin-plate spline), $\phi(r)=\mathrm{e}^{-ar^2}$, $\alpha>0$ (Gaussian), $\phi(r)=\sqrt{r^2+c^2}$ (multi-quadric), and $\phi(r)=1/\sqrt{r^2+c^2}$ (inverse multi-quadric). In this study, the multi-quadric formulation of RBF is used because of its prediction accuracy and its increasing rate of convergence with increased number of training points [**33**].

Given the locations $\boldsymbol{x}$ of training points and the calculated responses $y(\boldsymbol{x})$ at training points, the unknown interpolation coefficients λ_i are found by minimizing the residual R as

$$R=\sum_{j=1}^{N}\left[y(\boldsymbol{x}_j)-\sum_{i=1}^{N}\lambda_i\phi\left(\left\|\boldsymbol{x}_j-\boldsymbol{x}_i\right\|\right)\right]^2 \tag{2}$$

Equation (2) can be expressed in matrix form as

$$[A]\boldsymbol{\lambda}=\boldsymbol{y} \tag{3}$$

where $[A]=\left[\phi\left\|\boldsymbol{x}_j-\boldsymbol{x}_i\right\|\right]$, $i=1,\ldots,N$, $j=1,\ldots,N$, $\boldsymbol{\lambda}^{\mathrm{T}}=\{\lambda_1,\lambda_2,\ldots,\lambda_N\}^{\mathrm{T}}$, and $\boldsymbol{y}^{\mathrm{T}}=\{y(x_1),y(x_2),\ldots,y(x_N)\}^{\mathrm{T}}$. The unknown interpolation coefficient vector $\boldsymbol{\lambda}$ is obtained by solving equation (3).

3 CURRENT PRACTICE IN CHOOSING THE RBF PARAMETERS

As noted earlier, the choice of the shape parameter c has a substantial effect on the accuracy of the RBF model. Several researchers selected the shape variable c based on their experience or intuition. For instance, Wang *et al.* [**33**] noted that, if the radial distances between the training points are normalized to the range (0, 1), then $c=1$ works well for most problems. Similarly, Fang *et al.* [**20**] and Rais-Rohani *et al.* [**22**] used $c=1$ to predict the crash responses of automobiles and obtained satisfactory results.

It has been argued in many studies including those by Bogomolny [**34**] and Cheng *et al.* [**35**] that the accuracy of RBF models can be maximized by letting the shape parameter $c\to\infty$. This is true if there is no round-off error. Huang *et al.* [**36**] used a new error estimate that takes round-off error into account and proposed a new formulation for the optimal value of the shape parameter. Through numerical examples they showed that there is a finite and problem-dependent optimal value for the shape parameter c.

The most popular way of selecting an optimal value for the RBF shape parameter c is using the procedure proposed by Rippa [**29**], who selected the RBF shape parameter c by minimizing the r.m.s. CVE evaluated at training points. The optimization problem can be formulated as

$$\text{Find } c \tag{4.1}$$

$$\text{Minimize } E=\sqrt{\frac{1}{N}\sum_{k=1}^{N}\left[y_k-\hat{y}_{(k)}(c)\right]^2} \tag{4.2}$$

where E is the *global* CVE (r.m.s. CVE). The CVE at any training point is defined as $[y_k-\hat{y}_{(k)}(c)]$, where the term y_k is the true response at the kth training point $\boldsymbol{x}_k$, and the term $\hat{y}_{(k)}(c)$ is the prediction of an RBF model constructed using all except the kth training point. Obviously, the predicted value depends on the selected shape parameter c.

It has been shown that selecting the value of c based on minimization of the global CVE provides substantial accuracy improvement compared with selecting the value of c based on experience or intuition [**29–31**]. However, the accuracy of RBF models can be further improved by allowing the RBF shape parameters to take flexible values over the design space. This is discussed in the next section.

4 A NEW FORMULATION TO CHOOSE THE PARAMETERS

Instead of using a constant value for the shape parameter c over the entire design space, having a flexible c may allow the local behaviour to be captured better, thereby improving the accuracy. This can be easily achieved by allowing c to take different values at different training points; i.e. for any constructed RBF model, there exists a number N of c values c_1, c_2, …, c_N. Then, these shape parameters can be found by solving the optimization problem

$$\text{Find } c_1,c_2,\ldots,c_N \tag{5.1}$$

$$\text{Minimize } E=\sqrt{\frac{1}{N}\sum_{k=1}^{N}\left[y_k-\hat{y}_{(k)}(c_k)\right]^2} \tag{5.2}$$

where c_k is the value of c at the training point $\boldsymbol{x}_k$. The downside of this approach is that, as the number N of training points increases, the computational cost associated with optimizing the shape parameters can quickly escalate. Hence, this is not a good strategy. In this study, the shape parameter c is restricted to take a single value for any constructed RBF model, but for each training point a different RBF model is constructed; i.e. N different RBF models (with different but constant c_k) are constructed. Then, the predictions of N different RBF models are interpolated for the prediction point $\boldsymbol{x}$. With this procedure, the number of design variables for each RBF model is limited to one, while the flexibility of c over the design space is also maintained. The shape parameters of each of the N different RBF models are calculated by solving N times the optimization problem

$$\text{Find } c_k,\ k=1,\ldots,N \tag{6.1}$$

$$\text{Minimize } E_k = y_k - \hat{y}_{(k)}(c_k) \tag{6.2}$$

where E_k is the *pointwise* CVE evaluated at the kth training point, and c_k is the value of the shape parameter c that minimizes the pointwise CVE at the kth training point $\boldsymbol{x}_k$.

Then, the prediction of the response at $\boldsymbol{x}$ is evaluated from

$$\hat{y}(\boldsymbol{x}) = \sum_{k=1}^{N} \lambda_k \sqrt{\|\boldsymbol{x}-\boldsymbol{x}_k\|^2 + c(\boldsymbol{x})^2} \tag{7}$$

where the flexible shape parameters are calculated from

$$c(\boldsymbol{x}) = \sum_{\substack{k=1 \\ k\neq i}}^{N} \frac{c_k}{r_k(\boldsymbol{x})} \Bigg/ \sum_{\substack{k=1 \\ k\neq i}}^{N} \frac{1}{r_k(\boldsymbol{x})} \tag{8}$$

and $r_k(\boldsymbol{x})$ is the radial distance between $\boldsymbol{x}_k$ and the prediction point $\boldsymbol{x}$, which is computed from $r_k(\boldsymbol{x}) = \|\boldsymbol{x}-\boldsymbol{x}_k\|$. Note that the formulation of equation (8) is heuristic.

The proposed approach is based on constructing multiple RBF models and using equation (8) to interpolate the shape parameters. This approach is close to constructing an ensemble of metamodels, where different types of metamodel are constructed and combined in the form of an ensemble using a weighing scheme that assigns larger weights to more accurate metamodels. The reader is referred to the papers by Goel *et al.* [**37**], Acar and Rais-Rohani [**38**], and Viana *et al.* [**39**] for more information on the ensemble of metamodels.

5 TEST PROBLEMS

To evaluate the effectiveness of the proposed method of optimizing shape parameters of radial basis functions, first three benchmark mathematical functions are used. Then, the proposed method is applied to an automobile crash problem.

5.1 Benchmark mathematical problems

The following benchmark functions are used as part of the test problems in this study. These benchmark functions are taken from the book by Dixon and Szegö [**40**].

5.1.1 Branin–Hoo (two-variable) function

This is given by

$$y(x_1,x_2) = \left(x_2 - \frac{5.1x_1^2}{4\pi^2} + \frac{5x_1}{\pi} - 6\right)^2 + 10\left(1-\frac{1}{8\pi}\right)\cos(x_1) + 10 \tag{9}$$

where $x_1 \in [-5, 10]$ and $x_2 \in [0, 15]$. The Branin–Hoo function is depicted in Fig. 1.

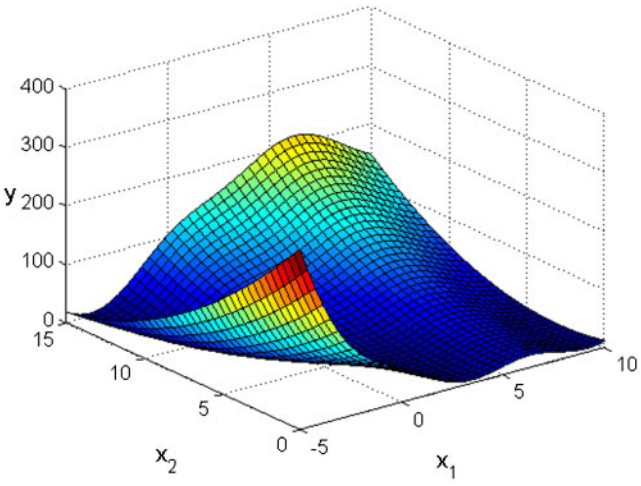

Fig. 1 Branin–Hoo function

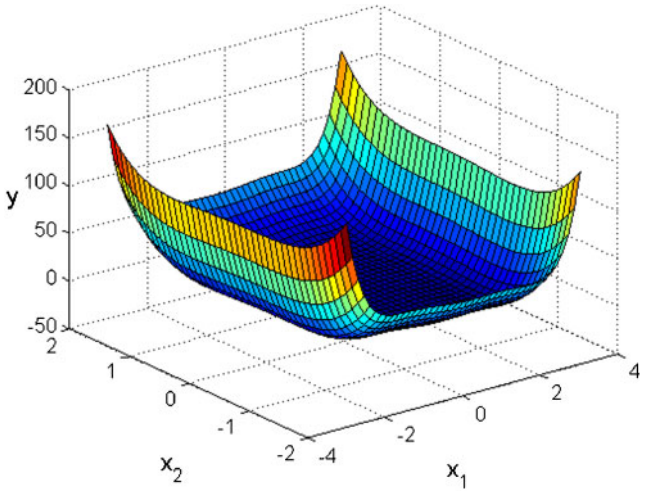

Fig. 2 Camelback function

5.1.2 Camelback (two-variable) function

This is given by

$$y(x_1, x_2) = \left(4 - 2.1x_1^2 + \frac{x_1^4}{3}\right)x_1^2 + x_1x_2 + \left(-4 + 4x_2^2\right)x_2^2 \tag{10}$$

where $x_1 \in [-3, 3]$ and $x_2 \in [-2, 2]$. The Camelback function is depicted in Fig. 2.

5.1.3 Hartman function (six-variable) function

This is given by

$$y(\boldsymbol{x}) = -\sum_{i=1}^{m} c_i \exp\left[-\sum_{j=1}^{n} a_{ij}\left(x_j - p_{ij}\right)^2\right] \tag{11}$$

where $x_i \in [0, 1]$. Here, a six-variable ($n = 6$) model of this function is considered, where m is taken to be equal to 4. The values of the function parameters c_i, a_{ij}, and p_{ij} are provided in Table 1.

5.2 Automobile crash problem

In the safety design of automobiles, crashworthiness considerations are particularly important. An automobile is designed such that particular crash responses (such as the intrusion of components into the driver compartment, and the accelerations at specified locations) need to be smaller than their allowable values. In this paper, full-frontal impact (FFI) of a c-class passenger car is investigated, whereas other possible crash scenarios such as offset-frontal impact, side impact, roof crash, and rear impact are not included.

An FE model of a c-class passenger car is used to simulate an FFI scenario using the FE code LS-DYNA. This FE model was also used in one of the studies in which the present author was involved [**41**]. It is a modified version of the full-scale FE model of a c-class passenger car developed by the Partnership for a New Generation of Vehicles [**42**]. The model consists of 313 components totalling a mass of approximately 1210 kg. The automobile components are modelled using isotropic materials with the non-linear behaviour of material defined by the true stress–strain curves at different strain rates.

The responses of interest are the intrusion distances and average peak accelerations at the floor pan, the driver seat, and steering-wheel locations (Fig. 3) for a crash duration of 100 ms. Overall, there are six responses of interest.

The input variables of the RBF models are the shape control parameters (x_1 to x_4) and the wall thickness (x_5) of the two side rails (Fig. 4) as well as the parameters that define variability or uncertainty in the material stress–strain relationship (x_6), offset distance (x_7), impact speed (x_8), and occupant mass (x_9). Overall, there are nine input variables.

6 THE NUMERICAL PROCEDURE

For the mathematical benchmark problems, Latin hypercube sampling (LHS) is used to select the locations of the training points as well as the test points such that the minimum distance between the points is maximized. The MATLAB built-in function 'lhsdesign' is used to generate the training and test points. Here, the 'maximin' criterion with a maximum of 100 iterations is used.

Table 1 Parameters used in the six-variable Hartman function, $j = 1, \ldots, 6$

	a_{ij} for the following j							p_{ij} for the following j					
i	$j=1$	$j=2$	$j=3$	$j=4$	$j=5$	$j=6$	c_i	$j=1$	$j=2$	$j=3$	$j=4$	$j=5$	$j=6$
1	10.0	3.0	17.0	3.5	1.7	8.0	1.0	0.1312	0.1696	0.5569	0.0124	0.8283	0.5886
2	0.05	10.0	17.0	0.1	8.0	14.0	1.2	0.2329	0.4135	0.8307	0.3736	0.1004	0.9991
3	3.0	3.5	1.7	10.0	17.0	8.0	3.0	0.2348	0.1451	0.3522	0.2883	0.3047	0.6650
4	17.0	8.0	0.05	10.0	0.1	14.0	3.2	0.4047	0.8828	0.8732	0.5743	0.1091	0.0381

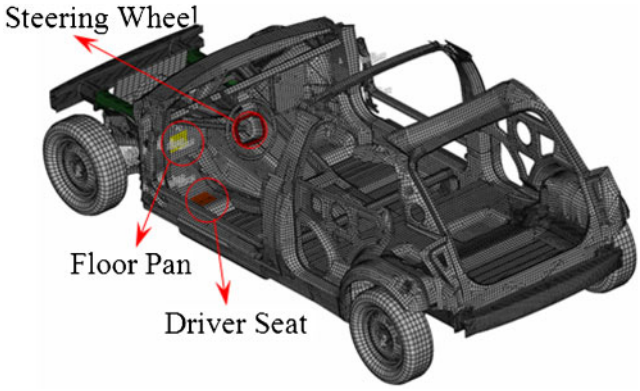

Fig. 3 Vehicle FE model showing the side rail and locations of measured responses [**41**]

To reduce the effect of random sampling, 1000 sets of training points are used for all the benchmark problems. For each set, 20 training points are used for the two-variable Branin–Hoo and Camelback functions, and 60 training points are used for the six-variable Hartman function. Hence, the RBF models are constructed multiple times with different training sets. To measure the prediction accuracy of the RBF models, 1000 sets of test points are generated. In each set, 1000 test points are used.

The RMSE is chosen as the error metric of interest. The average RMSE evaluated over 1000 different sets of test points is computed for the benchmark problems.

For the automobile crash problem, the LHS technique is also used. Owing to the large computational cost of FE simulations, however, the RBF models are constructed for only a single training set with 100 points, and the RMSE is computed over a single test set with 40 points, which are not among the 100 training points. Overall, 140 crash simulations are performed. Note that a single FE simulation takes about 13 central processing unit hours using a 32-processor IBM Linux Cluster with Intel Pentium III 1.266 GHz processors and 607.5 GB random-access memory (available at the Center for Advanced Vehicular Systems, Mississippi State University). A summary of the training and test sets information is provided in Table 2.

Table 2 Summary of training and test data used in each problem

Problem	Number of training and test sets	Number of points in a training set	Number of points in a test set
Branin–Hoo	1000	20	1000
Camelback	1000	20	1000
Hartman	100	60	1000
Automobile crash	1	100	40

7 RESULTS AND DISCUSSION

The effectiveness of the proposed method is evaluated on the basis of its ability to reduce the RMSE. The RMSE values are normalized with respect to the RMSE of RBF models constructed by using $c = 1$. Hereafter, the word 'normalized' is dropped when referring to the error.

7.1 Benchmark functions

For the Branin–Hoo and Camelback functions, RBF models are constructed using four different approaches:

(a) setting $c = 1$;
(b) selecting c using the Rippa method (c_Rippa);
(c) selecting c using the proposed method (c_Prop.);
(d) selecting c by solving the optimization problem stated in equation (5) (c_Eq. 5.2).

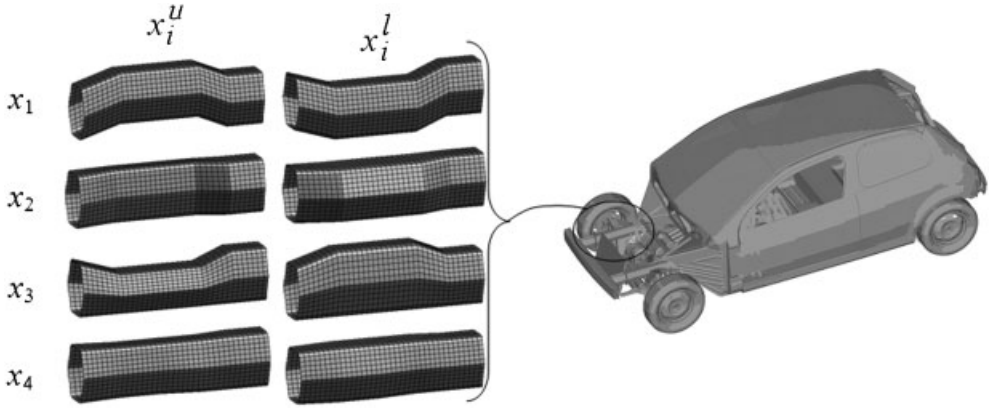

Fig. 4 Perturbed geometry of the right-hand side rail at the upper and lower limits of x_1 to x_4

Table 3 Comparison of the average RMSEs of the constructed RBF models with different shape parameter selection procedures for the benchmark functions

	Average RMSE*			
Problem	$c = 1$	c_Rippa	c_Prop.	c_Eq. 5.2
Branin–Hoo	1	0.79	**0.78**	0.86
Camelback	1	0.92	**0.89**	0.95
Hartman	1	0.84	**0.83**	Not computed†

*Average over 1000 different training and test sets.
†Owing to a larger computational cost.

Table 4 Comparison of the average CVEs of the constructed RBF models with different shape parameter selection procedures for the benchmark functions

	Average CVE*			
Problem	$c = 1$	c_Rippa	c_Prop.	c_Eq. 5.2
Branin–Hoo	1	0.65	0.72	0.09
Camelback	1	0.75	0.83	0.16
Hartman	1	0.79	0.82	Not computed†

*Average over 1000 different training and test sets.
†Owing to a larger computational cost.

For the six-variable Hartman function, solving the optimization problem stated in equation (5) would be computationally costly, and so only the first three methods mentioned above are used.

The results for the benchmark problems are provided in Tables 3 and 4 as well as Figs 5 to 10. In Table 3, the smallest error for each problem is indicated in bold for ease of comparison. Overall, the least accurate RBF models are constructed by setting $c = 1$. On average, the shape parameter selection based on the Rippa method reduces the error in RBF predictions by 21 per cent for the Branin–Hoo function, 8 per cent for the Camelback function, and 16 per cent for the Hartman function compared with the use of $c = 1$. The proposed method based on pointwise CVE further reduces the errors by an additional 1 per cent for the Branin–Hoo and the Hartman functions and an additional 3 per cent for the Camelback function. Selecting the shape parameter by solving equation (5) leads to the smallest CVE (as expected) as shown in Table 4, but it leads to larger RMSE values than both the Rippa method and the proposed method do. This finding arises because the setting for minimum CVE does not necessarily lead to minimum RMSE; even though CVE is usually a good surrogate for the actual error, the setting that minimizes CVE does not necessarily minimize the actual error.

Figure 5 shows the box plots for the RMSEs of the RBF models corresponding to the three different shape factor selection procedures for the Branin–Hoo function. The box plots show how the RMSE varies over the different training and test sets used. The bottom and top of each box represent the lower and upper quartile values respectively, with the interior line representing the median. The dashed lines (whiskers) extending from both ends of the box indicate the extents of the remaining data relative to the lower and upper quartiles. Here, the maximum whisker length is set at 1.5 times the inter-quartile range, and the data beyond this limit are characterized as outliers and represented by the plus symbols. The box plots for the RMSEs of the RBF models constructed for the Camelback function and the Hartman function are provided in Figs 6 and 7 respectively. Similarly, the box plots for the CVE of the RBF models constructed for the Branin–Hoo function, the Camelback function, and the Hartman function are depicted in Figs 8, 9, and 10 respectively.

The difference between the performances of the RBF models constructed on the basis of the global CVE minimization (the Rippa method) and the proposed method is very small in some of the example problems. It is not easy to decide from Figs 5 to 7 whether the results are statistically significant or not. To assess whether the proposed method performs better, a t test is performed for the RMSEs of the RBF models constructed using the proposed method and the RMSEs of the RBF models constructed using the Rippa method. Table 5 presents the degrees of freedom for the example problems, the corresponding critical t statistics, and the computed t statistics. It is seen that the computed t statistics are larger than the critical values for the Branin–Hoo and the Camelback functions, and smaller for the Hartman function. Therefore, the results of the Branin–Hoo and the Camelback functions are statistically significant, while those of the Hartman function are not. Note also that the negative values of the computed t statistics are indications that the average performance of the proposed method is better than that of the Rippa procedure.

7.2 Automobile crash problem

The results for the automobile crash problem are provided in Table 6. When the performances of RBF models for predicting intrusion distances or

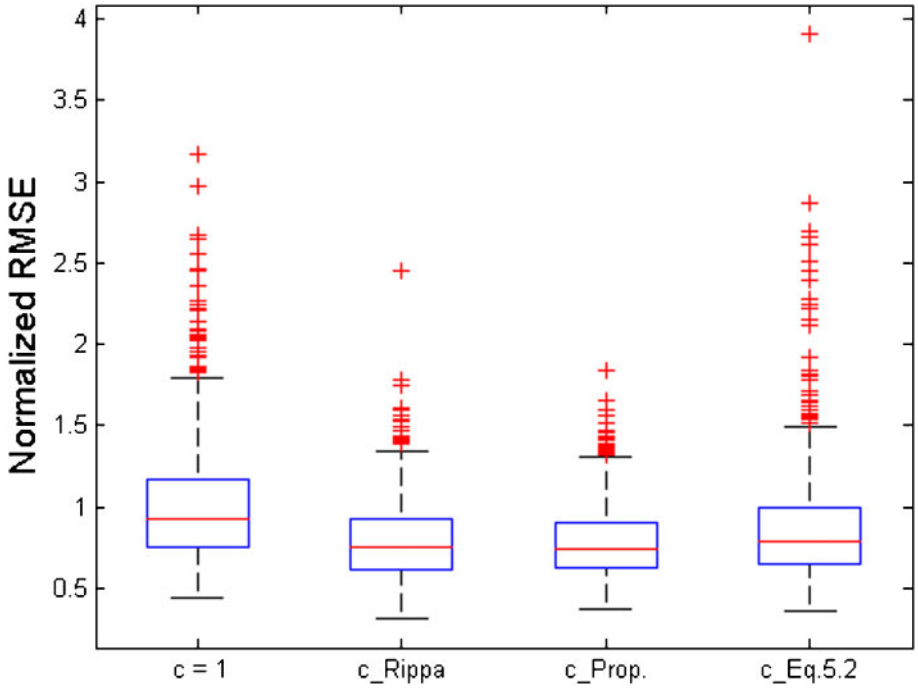

Fig. 5 Box plots of the normalized RMSE over 1000 training and test sets for the Branin–Hoo function

accelerations are compared, no clear superiority is observed for any model. Similarly, there is no clear distinction regarding the performances of the RBF models at different locations of the automobile.

The shape parameter selection based on global CVE minimization reduces the error in RBF predictions up to 18 per cent compared with the use of $c = 1$ for the different crash responses considered. The proposed pointwise shape para-

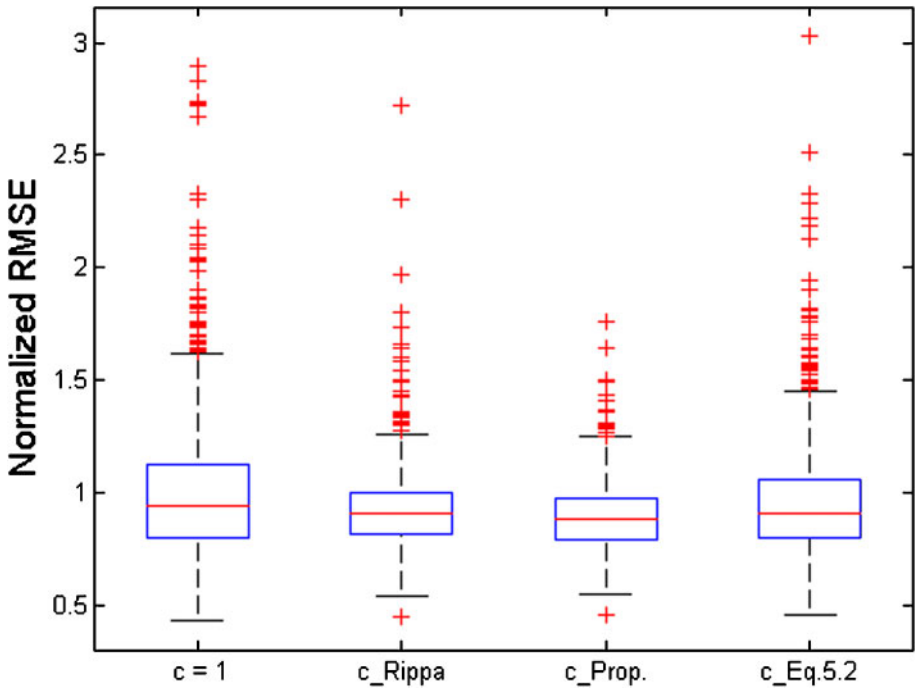

Fig. 6 Box plots of the normalized RMSE over 1000 training and test sets for the Camelback function

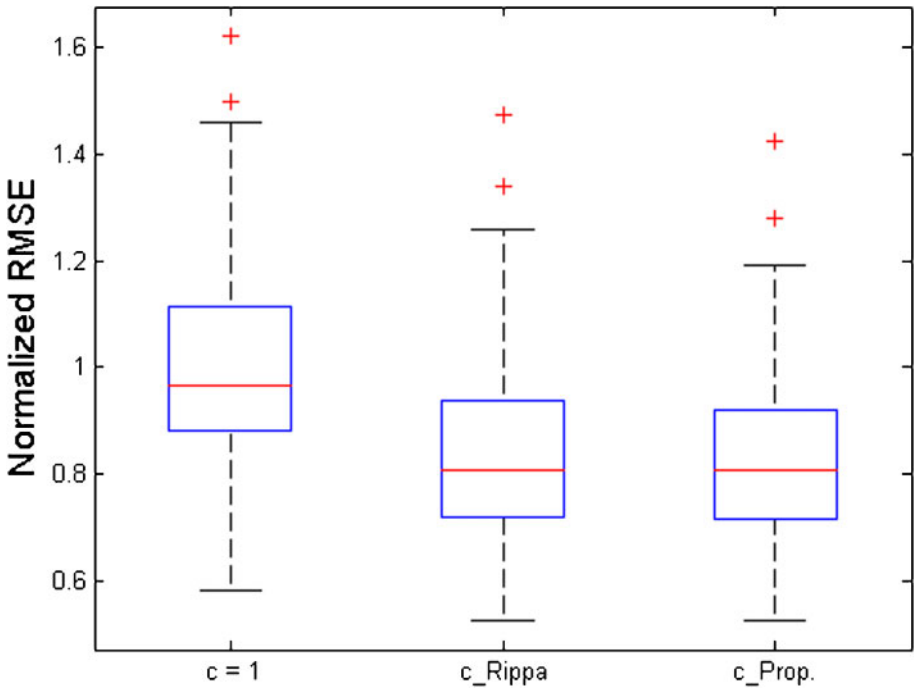

Fig. 7 Box plots of the normalized RMSE over 100 training and test sets for the Harman function

meter selection procedure further reduces the errors by 5–13 per cent. The only exception is for the acceleration at the steering wheel, where the error associated with the proposed procedure is 1 per cent larger than that of the global CVE minimization procedure.

8 CONCLUDING REMARKS

The most popular way of selecting the optimal RBF shape parameters is based on minimizing the global CVE. This paper proposed a methodology to optimize the RBF shape parameters based on minimiza-

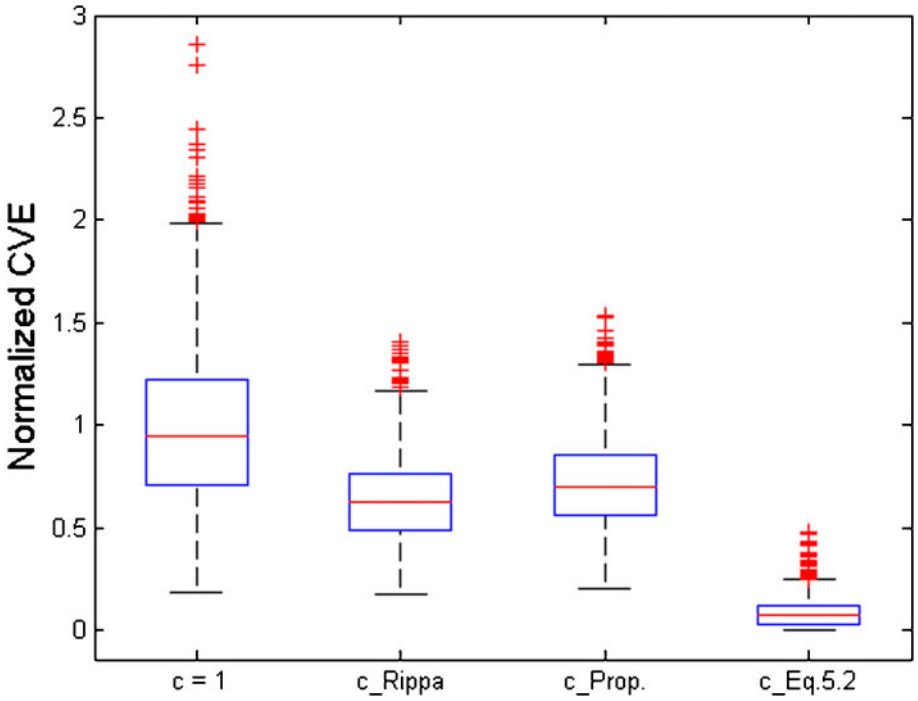

Fig. 8 Box plots of the normalized CVE over 1000 training sets for the Branin–Hoo function

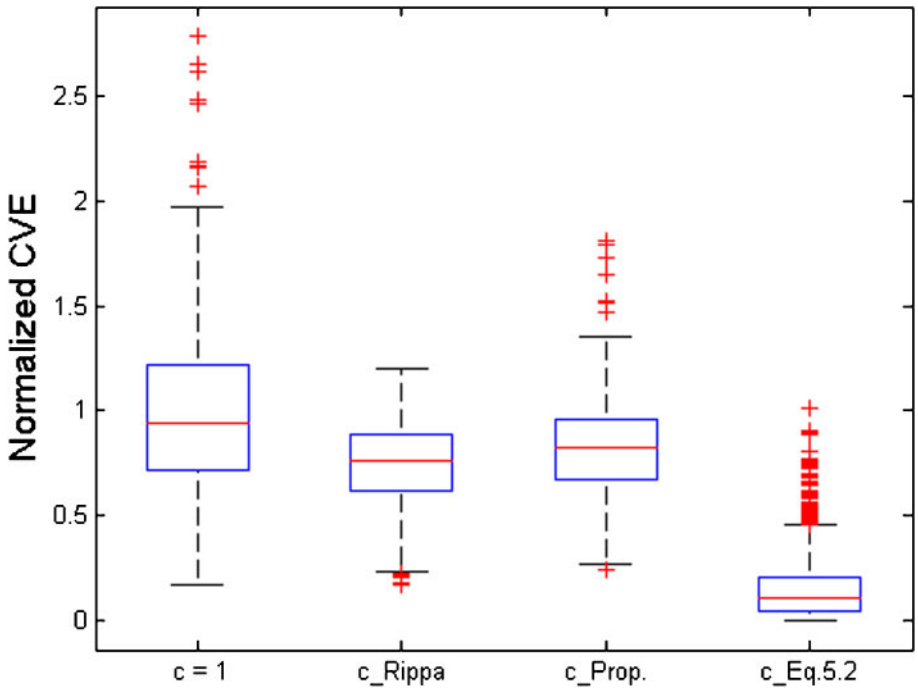

Fig. 9 Box plots of the normalized CVE over 1000 training sets for the Camelback function

tion of the pointwise CVE. Three benchmark mathematical problems and an automobile crash problem were used to evaluate the efficiency of the proposed method. From the results obtained in this study, the following were observed.

1. For the mathematical benchmark problems, the least accurate RBF models are constructed by setting $c = 1$. The shape parameter selection based on global CVE minimization (the Rippa method) reduced the error in RBF predictions by 8–21 per

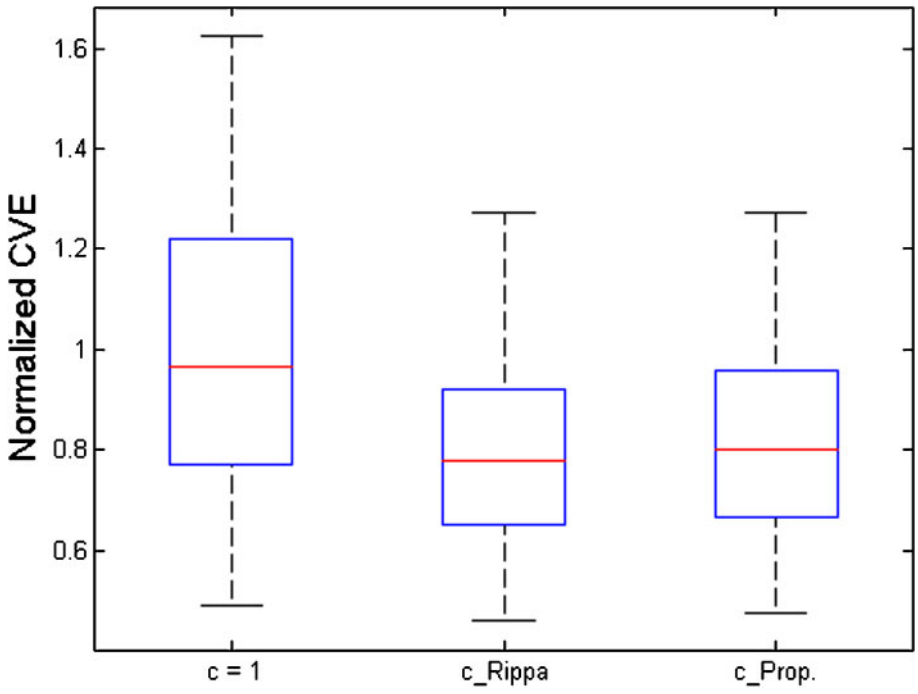

Fig. 10 Box plots of thenormalized CVE over 1000 training sets for the Hartman function

Table 5 Results of the *t* tests for the example problems

Problem	Degree of freedom	Critical *t*-statistic value for the $\alpha = 0.05$ confidence level	Computed *t*-statistic
Branin–Hoo	999	1.96	−2.15
Camelback	999	1.96	−6.48
Hartman	99	1.98	−0.88

Table 6 Comparison of the RMSEs of constructed RBF models with different shape parameter selection procedures for the automobile crash problem

	RMSE		
Response	$c = 1$	*c*_Rippa	*c*_Prop.
Intrusion distance at the floor pan	1	0.92	**0.88**
Intrusion distance at the driver seat	1	0.85	**0.78**
Intrusion distance at the steering wheel	1	0.98	**0.87**
Acceleration at the floor pan	1	1.00	**0.87**
Acceleration at the driver seat	1	0.98	**0.92**
Acceleration at the steering wheel	1	**0.82**	0.83

cent compared with setting the shape parameter to $c = 1$. The proposed method based on pointwise CVE minimization further reduced the errors by 1–3 per cent. In addition, for the Branin–Hoo function and the Camelback function, RBF models were also constructed by allowing the shape parameters to take different values at different data points and minimizing the global CVE. Even though this approach resulted in a smaller CVE than for the Rippa method and the proposed method, it led to larger RMSE values. This finding was explained with the reasoning that, even though CVE is usually a good surrogate for the actual error, the setting that minimizes CVE does not necessarily minimize the actual error.

2. For the automobile crash problem, greater error reductions were observed. The shape parameter selection based on global CVE minimization reduced the error in RBF predictions up to 18 per cent (for the different crash responses considered) compared with setting the shape parameter to $c = 1$. The proposed method based on pointwise CVE minimization further reduced the errors by 5–13 per cent, with the exception that the error for the acceleration reduction at the steering wheel increased by 1 per cent.

ACKNOWLEDGEMENTS

The author wishes to thank Dr Kiran Solanki at the Mississippi State University for performing the crash simulations used in this study. Also, the Center for Advanced Vehicular Systems, Mississippi State University, is acknowledged for sharing computational resources.

REFERENCES

1 **Mullur, A. A.** and **Messac, A.** Extended radial basis functions: more flexible and effective metamodeling. *AIAA J.*, 2005, **43**(6), 1306–1315.
2 **Hardy, R. L.** Multiquadric equations of topography and other irregular surfaces. *J. Geophys. Res.*, 1971, **76**, 1905–1915.
3 **Hardy, R. L.** Theory and applications of the multiquadric–biharmonic method. *Comput. Math. Applic.*, 1990, **19**(8–9), 163–208.
4 **Hardy, R. L.** A contribution of the multiquadric method: interpolation of potential inside the Earth: advances in the theory and applications of radial basis functions. *Comput. Math. Applic.*, 1992, **24**(12), 81–97.
5 **Arad, N., Dyn, N., Reisfeld, D.,** and **Yeshurun, Y.** Image warping by radial basis functions: applications to facial expressions. *Comput. Vision, Graphics, Image Processing*, 1994, **56**(2), 161–172.
6 **Tu, C. H.** and **Barton, R. R.** Production yield estimation by the metamodel method with a boundary-focused experiment design. In Proceedings of the ASME Design Theory and Methodology Conference, Sacramento, California, USA, 1997 paper DETC97/DTM3870 (ASME International, New York).
7 **Zala, C. A.** and **Barrodale, I.** Warping aerial photographs to orthomaps using thin plate splines. *Adv. Comput. Math.*, 1999, **11**, 211–227.
8 **Kremper, A., Schanze, T.,** and **Eckhorn, R.** Classification of neural signals by a generalized correlation classifier based on radial basis functions. *J. Neurosci. Meth.*, 2002, **116**, 179–187.
9 **Papila, N., Shyy, W., Griffin, L.,** and **Dorney, D. J.** Shape optimization of supersonic turbines using global approximation methods. *J. Propulsion Power*, 2002, **18**(3), 509–518.
10 **Reddy, R. R. K.** and **Ganguli, R.** Structural damage detection in a helicopter rotor blade using radial basis function neural networks. *Smart Mater. Structs*, 2003, **12**, 232–241.
11 **Lai, W., Tse, P. W., Zhang, G.,** and **Shi, T.** Classification of gear faults using cumulants and the radial basis function network. *Mech. Systems Signal Processing*, 2004, **18**(2), 381–389.
12 **Sonar, D. K., Dixit, U. S.,** and **Ojha, D. K.** The application of a radial basis function neural network for predicting the surface roughness in a turning process. *Int. J. Advd Mfg Technol.*, 2006, **27**, 661–666.

13 **Zhang, T., Choi, K. K., Rahman, S., Cho, K., Baker, P., Shakil, M.,** and **Heitkamp, D.** A hybrid surrogate and pattern search optimization method and application to microelectronics. *Struct. Multidisciplinary Optimization*, 2006, **32**(4), 327–345.

14 **Young, A., Cao, C., Patel, V., Hovakimyan, N.,** and **Lavertsky, E.** Adaptive control design methodology for nonlinear-in-control systems in aircraft application. *J. Guidance, Control Dynamics*, 2007, **30**(6), 1770–1782.

15 **Sjögren, D.** *Statistical methods for improving surrogate models in antenna optimization.* Master's Thesis, Chalmers University of Technology, Göteborg, Sweden, 2009.

16 **Jin, R., Chen, W.,** and **Simpson, T. W.** Comparative studies of metamodelling techniques under multiple modelling criteria. *Struct. Multidisciplinary Optimization*, 2001, **23**(1), 1–13.

17 **Chen, W., Garimella, R.,** and **Michelena, N.** Robust design for improved vehicle handling under a range of maneuver conditions. *Engng Optimization*, 2001, **33**(3), 303–326.

18 **Lanzi, L., Castelletti, L. M. L.,** and **Anghileri, M.** Multi-objective optimisation of composite absorber shape under crashworthiness requirements. *Composite Structs*, 2004, **65**, 433–441.

19 **Hamza, K.** and **Saitou, K.** Crashworthiness design using meta-models for approximating the response of structural members. In Proceedings of the Eighth Cairo University Conference on *Mechanical design and production* (*MDP-8*), Cairo, Egypt, 4–6 January 2004, vol. 1, pp. 591–602 (Cairo University, Cairo).

20 **Fang, A., Rais-Rohani, M., Liu, Z.,** and **Horstemeyer, M. F.** A comparative study of metamodeling methods for multiobjective crashworthiness optimization. *Comput. Structs*, 2005, **83**, 2121–2136.

21 **Yang, R. J., Wang, N., Tho, C. H., Bobineau, J. P.,** and **Wang, B. P.** Metamodeling development for vehicle frontal impact simulation. *J. Mech. Des.*, 2005, **127**(11), 1014–1020.

22 **Rais-Rohani, M., Solanki, K.,** and **Eamon, C.** Reliability-based optimization of lightweight automotive structures for crashworthiness. In Proceedings of the 11th AIAA/ISSMO Multidisciplinary Analysis and Optimization Conference, Portsmouth, Virginia, USA, 6–8 September 2006, AIAA paper 2006-7004 (AIAA, Reston, Virginia).

23 **Franke, R.** Scattered data interpolation: tests of some methods. *Math. Comput.*, 1982, **38**(157), 181–200.

24 **Kansa, E. J.** Multiquadrics – a scattered data approximation scheme with applications to computational fluid-dynamics – I surface approximations and partial derivative estimates. *Comput. Math. Applic.*, 1990, **19**(8–9), 127–145.

25 **Kansa, E. J.** Multiquadrics – a scattered data approximation scheme with applications to computational fluid-dynamics – II solutions to parabolic, hyperbolic and elliptic partial differential equations. *Comput. Math. Applic.*, 1990, **19**(8–9), 147–161.

26 **Fasshauer, G. E.** Newton iteration with multiquadrics for the solution of nonlinear PDEs. *Comput. Math. Applic.*, 2002, **43**(3–5), 423–438.

27 **Carlson, R. E.** and **Foley, T. A.** The parameter R^2 in multiquadric interpolation. *Comput. Math. Applic.*, 1991, **21**, 29–42.

28 **Foley, T. A.** Near optimal parameter selection for multiquadric interpolation. *J. Appl. Sci. Comput.*, 1994, **1**, 54–69.

29 **Rippa, S.** An algorithm for selecting a good value for the parameter c in radial basis function interpolation. *Adv. Comput. Math.*, 1999, **11**, 193–210.

30 **Wang, B. P.** Parameter optimization in multiquadric response surface approximations. *Struct. Multidisciplinary Optimization*, 2004, **26**, 219–223.

31 **Roque, C. M. C.** and **Ferreira, A. J. M.** Numerical experiments on optimal shape parameters for radial basis functions. *Numer. Meth. Partial Differential Equations*, 2010, **26**(3), 675–689.

32 **Buhmann, M. D.** *Radial basis functions: theory and implementations*, 2003 (Cambridge University Press, Cambridge).

33 **Wang, L., Beeson, D., Wiggs, G.,** and **Rayasam, M.** A comparison of meta-modeling methods using practical industry requirements. In Proceedings of the 47th AIAA/ASME/ASCE/AHS/ASC Structures, Structural Dynamics, and Materials Conference, Newport, Rhode Island, USA, 1–4 May 2006, AIAA paper 2006-1811 (AIAA, Reston, Virginia).

34 **Bogomolny, A.** Fundamental solutions method for elliptic boundary value problems. *SIAM J. Numer. Analysis*, 1985, **22**, 644–669.

35 **Cheng, A. H. D., Golberg, M. A., Kansa, E. J.,** and **Zammito, G.** Exponential convergence and *h–c* multiquadric collocation method for partial differential equations. *Numer. Meth. Partial Differential Equations*, 2003, **19**(5), 2003, 571–594.

36 **Huang, C. S., Lee, C. F.,** and **Cheng, A. H. D.** Error estimate, optimal shape factor, and high precision computation of multiquadric collocation method. *Engng Analysis Boundary Elements*, 2007, **31**, 614–623.

37 **Goel, T., Haftka, R. T., Shyy, W.,** and **Queipo, N. V.** Ensemble of surrogates. *Struct. Multidisciplinary Optimization*, 2007, **33**(3), 199–216.

38 **Acar, E.** and **Rais-Rohani, M.** Ensemble of Metamodels with optimized weight factors. *Struct. Multidisciplinary Optimization*, 2009, **37**(3), 279–294.

39 **Viana, F. A. C., Haftka, R. T.,** and **Steffen, V.** Multiple surrogates: how cross-validation errors can help us to obtain the best predictor. *Struct. Multidisciplinary Optimization*, 2009, **39**(4), 439–457.

40 **Dixon, L. C. W.** and **Szegö, G. P.** *Towards global optimization 2*, 1978 (North-Holland, Amsterdam).

41 **Rais-Rohani, M., Solanki, K., Acar, E.,** and **Eamon, C. D.** Shape and sizing optimization of automotive structures with deterministic and probabilistic design constraints. *Int. J. Veh. Des.*, 2010 (in press).

42 Partnership of a New Generation of Vehicles, ULSAB-AVC Program, May 1999, available from http://www.corusautomotive.com/file_source/automotive/Publications/ULSAB-TTD1.pdf.

APPENDIX

Notation

c	shape parameter of the radial basis function model
CVE	cross-validation error
E	r.m.s. cross-validation error (i.e. the global cross-validation error)
E_i	pointwise cross-validation error at the ith training point
N	number of training points
$\boldsymbol{r}_k(\boldsymbol{x})$	radial distance between the kth training point $\boldsymbol{x}_k$ and the prediction point $\boldsymbol{x}$
RMSE	r.m.s. error
$y(\boldsymbol{x})$	true value of the response evaluated at $\boldsymbol{x}$
$\hat{y}(\boldsymbol{x})$	radial basis function model prediction of the response $y(\boldsymbol{x})$ evaluated at $\boldsymbol{x}$
y_k	true response value at the kth training point
$\hat{y}_{(k)}$	predicted value of the response by the radial basis function model constructed using all except the kth training point
$\boldsymbol{\lambda}$	interpolation coefficients used in the radial basis function models
ϕ	radially symmetric basis function